The Rheology of Dense Colloidal Pastes Used in 3D-Printing

Michael P. Avery,[1,2] Susanne Klein,[3] Robert Richardson,[2] Paul Bartlett,[2] Guy Adams,[3] Fraser Dickin,[3] Steve Simske[4]
[1]Bristol Centre for Functional Nanomaterials (UK), [2]University of Bristol (UK), [3]HP labs Bristol (UK), [4]HP Labs Fort Collins (USA)

Abstract

The rheology of dense, aqueous pastes of soda-lime glass frit and a polysaccharide binder, designed for use in a recently developed glass 3D-printing process, is reported. Pastes containing either xanthan gum or 2-hydroxyethyl cellulose binder and glass frit with average particle sizes of either 38 – 63 µm or 150 – 250 µm were investigated using a controlled stress rheometer over an applied stress range of (10.66 – 942.2 Pa). The pastes exhibited yield behaviour followed by shear-thinning as the applied stress was increased, in a similar manner to highly concentrated polysaccharide solutions. The yield stress was found to be reduced for pastes containing xanthan gum binder and larger glass particles.

The physical properties (Young's modulus, opacity and density) of glass produced by kiln-firing pastes used for glass 3D-printing are also reported. Paste composition was varied to investigate the effect of micro scale changes on the macro scale glass properties. The average glass particle diameter in the frit was varied in the range 38 – 250 µm and glass produced from 'pastes' containing frit-only, frit with binder and frit with binder and water were compared.

Introduction

3D-printing, along with other additive manufacturing (AM) and rapid prototyping (RP) techniques, involves building up structures in a layer by layer fashion based upon a computer design file. Such techniques are well suited to the production of one-off, complex structures that would often be difficult to produce using traditional manufacturing methods. There has been rapid growth and interest in this field during recent years and a range of techniques are now available which make use of many common materials such as plastic, metal, wood and ceramic.[1] However, relatively little has been done to develop AM using glass.[2]

Klein *et al.*[3], [4] have built upon the work of previous powder-bed printing techniques[2] by developing an extrusion-based method of glass printing. This overcomes the weaknesses of the powder-bed method, such as the large volume of powdered material which must be held as a reservoir and the limitation to a single colour or material per printing cycle. The extrusion method uses dense aqueous pastes, containing glass frit and a polysaccharide binder, which are extruded into the desired shape using an adapted 3D-printer and then air-dried to form greenware. The greenware is then kiln-fired to fuse the glass particles and burn away the biopolymer binder.

Klein *et al.* found that, as expected, using frit with smaller average particle diameters improved print resolution. However, this also increased print opacity. This is believed to be the result of an increased number of gas inclusions in the prints acting to scatter light. The presence of pores within the glass could also have a detrimental effect on the mechanical properties. Increased porosity is, for example, linked to a reduction in the Young's modulus of an object, with as little as 10% porosity by volume predicted to reduce the Young's modulus by 20-40%, depending upon the theory used.[5] Ideally a printed glass object would have high resolution and transparency and mechanical properties comparable with those of glass produced by other methods and so efforts are being made to reduce the proportion of gas remaining in the final print.

Our approach to this problem is to increase the solid content of the printing pastes by improved particle packing. The use of bimodal particle distributions (two sets of particles with average diameters different by an order of magnitude) has been shown to increase the density of aqueous slurries used in slip-casting of ceramics.[6]–[8] This approach takes inspiration from ideal Apollonian packing where ever smaller spheres fill the gaps remaining between closely packed larger spheres.[9] The level of density increase in bimodal systems is found to depend upon the size ratio and the relative proportions of the two particle sizes;[10] however, it has been suggested that particle packing fractions in randomly close packed systems, such as those likely to be found in printing pastes, could reach up to 0.829.[11]

While it is important to maximize the packing density of particles in 3D-printed greenware, for a paste to be useful for extrusion printing it must also have favourable rheology. Pastes must be able to be extruded under applied force but have a low flow rate (high viscosity) once printed. This behavior is described as shear-thinning. For bimodal systems, viscosity is found to increase with increased solid loading while shear thinning characteristics are found to depend upon the particle size distribution and the ratio of coarse to fine particles.[6], [8], [12]

The role of the binder must also not be overlooked. From research on paste extrusion, it has been found that the rheology of pastes is closely linked to the rheology of the binder.[13], [14] The chosen binder for the printing pastes must therefore have shear-thinning properties in order to produce a successful print. Polysaccharide binders, such as those used by Klein *et al.*, are known to have shear-thinning properties in concentrated aqueous solutions[15]–[17] and are therefore expected to impart shear-thinning behaviour to the pastes under investigation in this work.

To optimise 3D-printing pastes, a balance will therefore need to be struck between maximal solid loading and favourable paste rheology, for a given paste system. To fully understand these macroscopic system properties a deeper understanding of the packing and distribution of particles at the micro and nanoscale is required, including: surface chemistry and interactions, the nature of particle mixing and the flow and rearrangement of particles under shear.

Within this paper we describe initial efforts to characterise the components of the glass printing system developed by Klein *et al.* in order to understand how paste composition influences paste extrusion and the properties of the final kiln-fired glass objects. We focus on the viscosity as a function of applied stress for the

3D-printing pastes and the properties of Young's modulus, opacity, and density for the kiln-fired glass samples.

Methodology

Materials

Powdered glass frit (soda-lime-silica) 'Crystal Clear', 'Clear' and 'Woodland Brown' was provided by Bullseye Glass. 2-Hydroxyethylcellulose, methylcellulose and xanthan gum was supplied by Sigma Aldrich and used as supplied. Any water used was Millipore filtered unless otherwise stated. The glass powder frit was sieved using an Endecotts Minor Sieve Shaker. The resulting frit size ranges will be denoted by a number as given in Table 1.

Table 1 – Numerical notation of the average particle diameter present in the glass frit.

Notation	Average particle diameter (Φ) in Frit
1	250 μm > Φ > 150 μm
2	150 μm > Φ > 75 μm
3	75 μm > Φ > 63 μm
4	63 μm > Φ > 38 μm
5	38 μm > Φ

Preparation of Glass Pastes

Using 'Clear' glass frit, pastes were produced according to methods developed by Klein *et al.*[3], [4] to investigate the effect of particle size and binder choice on paste viscosity. Two binders, xanthan gum (XG) and 2-hydroxyethylcellulose (HEC), were chosen as suitable binders based upon previous work.[3] The glass particles and binder were thoroughly mixed before the gradual addition of water, again while mixing. Mixing was performed by hand. Table 2 describes the pastes produced.

Table 2– Composition of the pastes used for rheology experiments.

Paste #	Frit Size	Binder	Glass:H_2O:Binder
1	(1)	XG	1:1:0.05
2	(5)	XG	1:1:0.05
3	(1)	HEC	1:1:0.05
4	(5)	HEC	1:1:0.05

Preparation and Firing of Greenware

Glass pellets used in SEM studies were produced using pastes containing Woodland Brown frit, methylcellulose and water in the ratio 2:1:0.1 using frit sizes 1, 2, 4 and 5. The pastes were shaped into pellets (4 mm thick and 8 mm diameter) and allowed to dry to form greenware.

Uniformly shaped glass samples (15 mm by 15 mm by 2 mm) were produced using rectangular moulds, to maintain sample shape during firing, and then post-processed after firing to cut the sample to uniform dimensions. This left the samples with a ground-glass finish. The composition of the samples is given in Table 3 while the denotation of frit particle size is given in Table 1. For example, sample CF1 would contain only Crystal Clear frit with an average particle diameter (Φ) of 250 μm > Φ > 150 μm.

All samples were fired according to the following schedule: (1) temperature ramp of 200°C/h to 150°C then hold for 5 minutes, (2) temperature ramp of 430°C/h to 720°C then hold for 10 minutes (3) full cool to 510°C and hold for 30 minutes (4) cool at rate of 80°C/h to 430°C and hold for 10 minutes (5) cool to room temperature.

Table 3 – Material composition of pre-fired uniformly shaped glass samples, given as a ratio by weight of each component.

Sample	'Crystal Clear' Frit	HEC	H_2O	'Crystal Clear' Billet
CF	1	-	-	-
FH	1	0.05	-	-
FHW	1	0.05	1	-
BL	-	-	-	1

Characterisation Techniques

The rheology of the glass pastes was measured using a Bohlin CS controlled stress rheometer with parallel plate geometry (25 mm diameter), calibrated using standard viscosity oils. Stress viscometry measurements were performed over an applied shear stress range of 10.66 - 942.2 Pa at 25°C.

The density of fired samples was determined using a pycnometer method[18] using deionised water. The error in a measurement was determined by the maximum deviation from the mean of 10 measurements of a single sample.

Images of the external surface and the internal structure of glass pellet samples were produced using a JEOL JSM 5600LV Scanning Electron Microscope (SEM). Characterisation of the internal structure was achieved by imaging fractured sample surfaces.

Light transmission data for the uniform fired glass samples was produced using an Ocean Optics spectrometer USB 2000 + and a halogen light source, 350 – 1100 nm wavelength range. To remove the effect of surface scattering the samples were tested while immersed in an index matching fluid (immersion oil for microscopy n20/D = 1.517 supplied by Sigma Aldrich). A transmission measurement through immersion oil was used as a background to all measurements.

A pulse-echo ultrasound technique was used to determine the Young's modulus of the uniform fired glass samples. This technique is a non-destructive alternative to traditional tensile and compression testing.[19] For an isotropic material, the Young's modulus (E) may be determined from the relationship between the longitudinal and transverse wave velocity within the glass.[19]–[21] Measurements were performed using an Agilent Technologies DSO1024A Oscilloscope 200 MHz 2 GSa/s and Olympus Pulser/Reciever with 5 MHz longitudinal and 5 MHz transverse transducers. Ultrasound coupling gel and golden syrup were used to ensure good contact with the longitudinal and transverse transducer respectively. Sample thicknesses were measured using a digital micrometer. Multiple echoes were recorded per sound pulse and the error in time of flight was determined from the standard deviation in the time between echoes. ΔE was determined using standard error combination formulas.

Results and Discussion

Paste Rheology

The results of stress viscometry measurements are shown in Figure 1 below. The printing pastes show very high viscosity at low applied shear stresses, exhibiting solid-like behavior, before yielding and then shear-thinning as the applied stress increased. These are exactly the rheological properties required for a successful printing paste which must shear-thin under pressure (pass easily through the print nozzle) but hold the printed shape once pressure is released. These properties were expected based upon observations of the pastes when in use in the printing system.

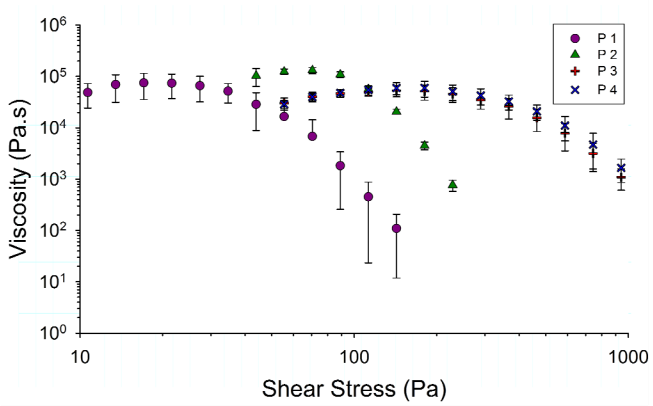

Figure 1 *– Stress viscometry measurements for pastes 1-4 (Table 2) comparing the effects of binder type and glass particle size used in the paste on the paste rheology.*

The general trends in viscosity follow those observed in highly concentrated solutions of polysaccharides which have a yield stress followed by a region of shear-thinning behavior as the applied stress is increased.[15]–[17] Given the high concentration of polysaccharide binders in the pastes and evidence that the flow properties of pastes are closely related to their constituent binder,[13], [14] it is hardly surprising that similar rheological behavior is observed.

The value of the yield stress is found to vary based upon the paste composition with pastes containing xanthan gum binder yielding at lower applied stress. Pastes containing large particles, with either binder, are also found to have a reduced yield stress, although this effect is less pronounced for HEC containing pastes.

If we assume that the dominant factor in the paste rheology derives from the binder rheology then we could explain these size effects as a result of the distribution of binder throughout the pastes. As the pastes contain the same ratio of binder to glass frit by mass, the pastes containing smaller particles will have a larger particle surface area. The thickness of the binder layer around the particles will therefore be reduced for the smaller particles as a larger surface area must be covered. Using a model proposed by Benbow *et al.*[14] for work on paste extrusion, there will be a certain critical value (V*) of binder required to just fill the interparticle voids. At values above V* extrusion becomes possible. As the thickness of the layer around the particles increases, the force required to extrude the paste will be reduced. Therefore, it could be argued that this increased yield stress for pastes containing smaller particles is as a result of the reduced thickness of the binder around each particle. This is, however, a very simplistic model, as Benbow *et al.* admit, and in fact it is more likely that rheological behaviour of pastes depends on a number of factors: amount of liquid/binder present beyond V*, the rheology of the liquid phase and interference between particles.

Understanding the rheology of the 3D-printing pastes is therefore a complex task requiring careful further study but, as a result of this work, we find that we can control and optimise the yield stress and hence the applied stress required for printing via the choice of binder and glass particle size used.

Kiln-fired Glass

The effect of particle size on the opacity of the glass samples can be clearly seen in Figure 2. Samples produced using smaller glass particles in the frit are found to exhibit greater opacity than those produced using larger glass particle sizes.

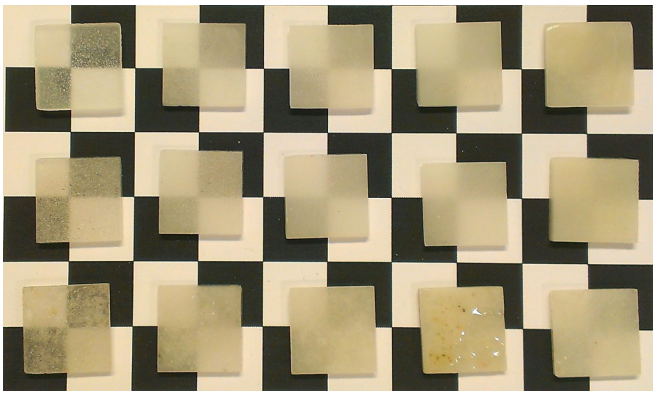

Figure 2 *– Photograph of uniform glass samples, all samples have a ground-glass finish as a result of post-processing methods. CF (top), FH (middle), FHW (bottom). Particle sizes 1-5 going from left to right. The increased opacity with decreasing particle size can be clearly observed.*

Light transmission measurements (Figure 3) quantify this observation, showing that all samples exhibit at least a 40% decrease in light transmission when compared to the standard soda-lime glass sample (BL), with further decreases in transmission as particle size decreases. The CF measurements show that a change in the glass structure must occur by simply breaking up and reforming glass in a kiln-fired process. We believe this change is shown by the presence of bubbles in the glass observed in Figure 2. This links with the theory that decreasing particle size increases the number of bubbles (light scatterers) and increases opacity. FH and FHW measurements show additional decreases in light transmission which may be linked to the presence of binder residues in the glass, indicated by the sample discolouration seen in Figure 2.

SEM images of glass pellets show a closed-pore internal structure, indicating the presence of bubbles, and a smooth, sealed outer surface (Figure 5). The smooth outer surface but porous interior is evidence of the surface of the sample sealing during the

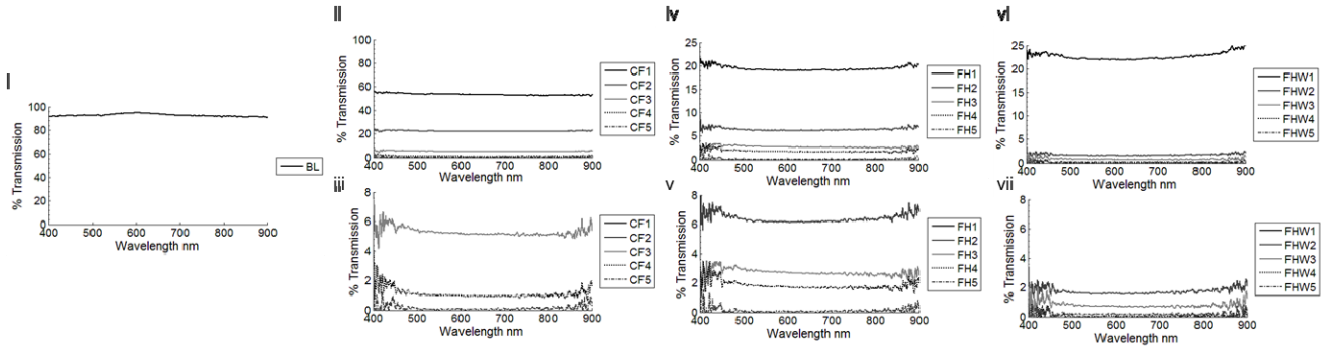

Figure 3 *– Light transmission measurements for fired glass samples CF (ii and iii), FH (iv and v) and FHW (vi and vii) measured whilst immersed in refractive index matching fluid, compared to standard glass sample, BL (i). iii, v, and vii show the lower transmission regions in greater detail for sample types BL, CF, FH, and FHW respectively. Note the variation in the y-axis scales.*

firing process, as a result of the external heat source, and trapping any remaining gas within the sample.

The presence of pores within the internal structure corresponds well with the bubbles observed in Figure 2 and the images allow us to make tentative comparisons between glass produced using different particle sizes. Samples produced using larger particle sizes show pore structures containing fewer but larger pores while samples produced using smaller frit sizes appear to have more pores which have a smaller average size. From this evidence, a change in pore size and distribution rather than an increase in the total pore volume could be the cause of changing sample opacity. However, these images only provide a 2D slice through a section of the sample structure, so further evidence would be required to confirm this assessment.

Density measurements (Figure 4) on CF, FH and FHW samples correspond well with the expected value for standard soda-lime glass[22] (2.5 g/cm^3), with the majority of samples having density values within the range 2.3 - 2.5 g/cm^3. The density of the standard samples (BL) of the same glass type as CF, FH and FHW, was found to be slightly below the expected value of 2.5 g/cm^3 and so the slightly reduced density values across all sample types is likely to be, in part, as a result of this.

Unfortunately the variance of the errors in the measurements make it very difficult to identify a trend in the sample density as a function of frit particle size. Ideally, density changes (or lack of) between samples would determine whether particle size influences the total porosity or instead the distribution of porosity as suggested by SEM micrographs.

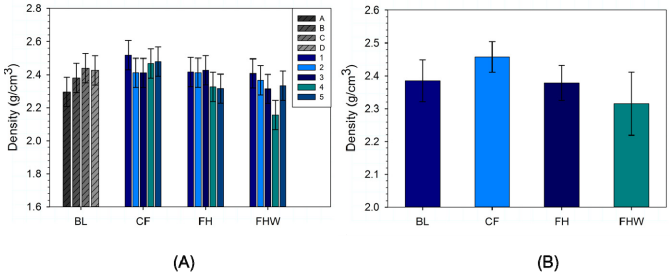

Figure 4 *– (A) Density values, produced using a pycnometry method, for fired glass samples CF, FH and FHW (1-5), compared to the density of four samples (A-D) of standard glass, BL. (B) Average density for each sample type. Error bars are standard deviation of samples 1-5, A-D for each sample type as appropriate. Sample details are given in Table 1 and Table 3.*

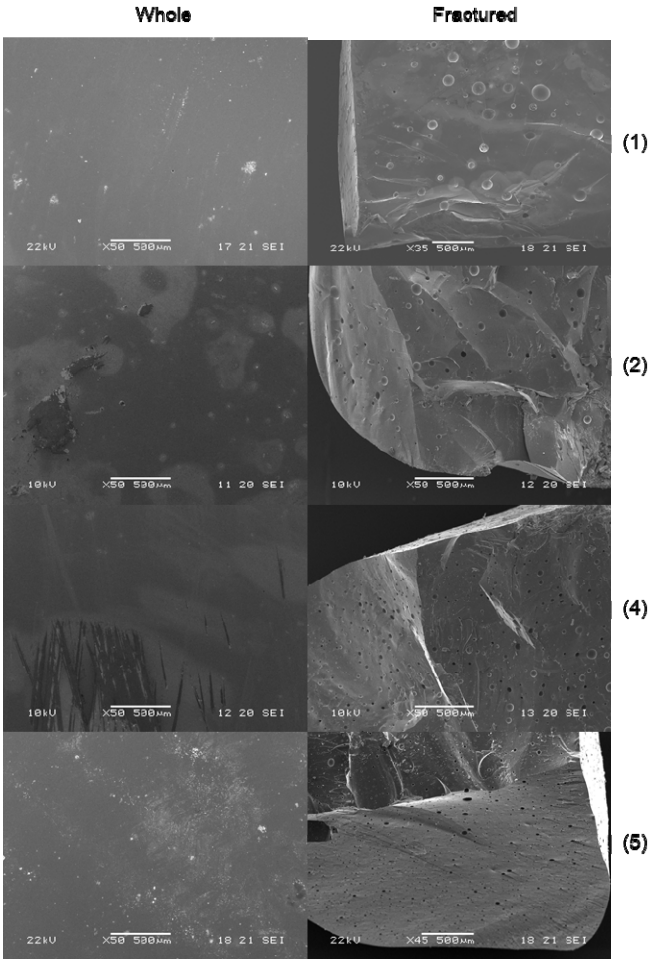

Figure 5 *– SEM micrographs of the external and internal structures of fired glass pellets. Internal structure observed along fractures in the samples. All scale bars represent 500 µm, magnification is 50x for all images other than (1) fractured (35x) and (5) fractured (45x).*

The mean Young's modulus values of the fired samples (CF, FH, FHW) are lower than for the standard glass (BL) (Figure 6B). It is well known that the Young's modulus of a material will decrease with increasing porosity and so it seems likely that the porosity, observed visually and via SEM, is the cause of this drop in E for the fired samples.[5], [23] The ratios of the Young's modulus values for the fired samples E_p to the Young's modulus of the standard glass E_0 give values of $E_p/E_0 = 0.944$, 0.945, 0.919 for CF, FH and FHW respectively. Based on theoretical models relating porosity to E, these values correspond to sample porosities of < 5% of the total volume.[5] This low level of porosity corresponds well with the isolated closed-pore structures observed by SEM.

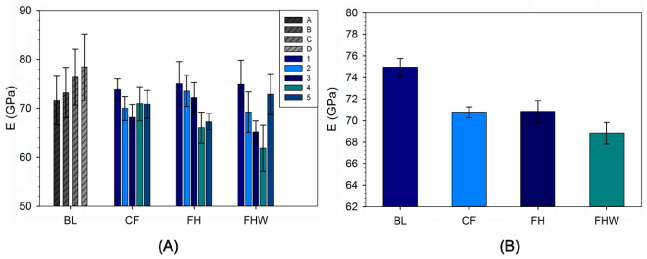

***Figure 6** – (A) Young's modulus values, produced using pulse-echo ultrasound testing, for fired glass samples CF, FH and FHW (1-5), compared to standard glass samples, BL (A-D). (B) Average Young's modulus values for each sample type. Errors are standard deviation of samples 1-5, A-D for each sample type as appropriate. Sample details are given in Table 1 and Table 3.*

Once again it is difficult to identify trends in E with changing particle size (Figure 6A), however all values lie in the range 60-80 GPa in good agreement with the expected Young's modulus of soda-lime glass (72 GPa).[22], [24] This agrees well with the density measurements and SEM evidence which show that all samples are primarily composed of soda-lime glass with any voids or residues contributing only a small percentage of the total material. Hence, there are only small variations from the expected value.

Summary

The rheology of 3D-printing pastes was found to follow the behaviour of the polysaccharide binder component as expected. The pastes behaved in a solid-like manner at low applied shear stress, then yielding and shear-thinning as the applied stress was increased. The value of the yield stress was found to depend on the choice of binder and particle size with lower yield stresses occurring for larger particle sizes and xanthan gum binder. This shows that through careful paste design, paste rheology can be controlled and modified to better suit 3DP applications.

Initial characterisation of the kiln-fired glass samples and the 3D-printing pastes used in the glass printing system developed by Klein *et al.* has shown that small changes in paste composition can greatly affect the macroscopic properties of both the pastes and the resulting glass prints. Pore structure, linked to glass particle size, is found to be of key importance to the mechanical and optical properties of the fired glass and as such is a major area of interest for the improvement of these printing systems. Understanding how particle size and packing are linked to different pore structures will therefore form the basis of our further work in this area.

Acknowledgements

MPA would like to thank: Dr. Cheryl Flynn for guidance with rheology, Prof. Bruce Drinkwater and Mr Philip Bassindale for access to, and support with, pulse-echo ultrasound testing equipment, Mr John Rowden and the School of Physics glass workshop for the post-processing of the uniform glass samples, Miss Shelley Taylor for help with MATLAB coding, the Soft Matter Group, the Richardson Group, the School of Chemistry Electron and Scanning Probe Microscopy Facility, the Bristol Centre for Functional Nanomaterials and also Hewlett Packard for funding this project.

References

[1] K. V. Wong and A. Hernandez, "A Review of Additive Manufacturing," *ISRN Mech. Eng.*, vol. 2012, pp. 1–10, 2012.

[2] G. Marchelli, R. Prabhakar, D. Storti, and M. Ganter, "The guide to glass 3D printing: developments, methods, diagnostics and results," *Rapid Prototyp. J.*, vol. 17, no. 3, pp. 187–194, 2011.

[3] S. Klein, F. Dickin, G. Adams, and S. Simske, "Glass : an old material for the future of manufacturing," *HP Tech Rep.*, 2012.

[4] S. Klein, S. Simske, C. Parraman, P. Walters, D. Huson, and S. Hoskins, "3D Printing of Transparent Glass," *HP Tech Rep.*, 2012.

[5] J. a. Choren, S. M. Heinrich, and M. B. Silver-Thorn, "Young's modulus and volume porosity relationships for additive manufacturing applications," *J. Mater. Sci.*, vol. 48, no. 15, pp. 5103–5112, Apr. 2013.

[6] G. Tari, J. Ferreira, A. Fonseca, and O. Lyckfeldt, "Influence of particle size distribution on colloidal processing of alumina," *J. Eur. Ceram. Soc.*, vol. 18, pp. 249–253, 1998.

[7] J. Zheng, W. B. Carlson, and J. S. Reed, "The packing density of binary powder mixtures," *J. Eur. Ceram. Soc.*, vol. 15, no. 5, pp. 479–483, Jan. 1995.

[8] S. . Olhero and J. M. . Ferreira, "Influence of particle size distribution on rheology and particle packing of silica-based suspensions," *Powder Technol.*, vol. 139, no. 1, pp. 69–75, Jan. 2004.

[9] S. Anishchik and N. Medvedev, "Three-dimensional apollonian packing as a model for dense granular systems," *Phys. Rev. Lett.*, vol. 75, no. 23, pp. 4314–4317, 1995.

[10] R. J. Hellmig and H. Ferkel, "Using Nanoscaled Powder as an Additive in Coarse-Grained Powder," *J. Am. Ceram. Soc.*, vol. 84, no. 2, pp. 261–66, Dec. 2004.

[11] A. B. Hopkins, F. H. Stillinger, and S. Torquato, "Disordered strictly jammed binary sphere packings attain an anomalously large range of densities," *Phys. Rev. E*, vol. 88, no. 2, p. 022205, Aug. 2013.

[12] S. . Olhero and J. M. . Ferreira, "Particle segregation phenomena occurring during the slip casting process," *Ceram. Int.*, vol. 28, no. 4, pp. 377–386, Jan. 2002.

[13] Z. C. Chen, "Effect of particle packing on extrusion behavior of pastes," vol. 5, pp. 5301–5307, 2000.

[14] J. Benbow, S. Blackburn, and H. Mills, "The effects of liquid-phase rheology on the extrusion behaviour of paste," *J. Mater. Sci.*, vol. 3, pp. 5827–5833, 1998.

[15] K.-W. Song, Y.-S. Kim, and G.-S. Chang, "Rheology of concentrated xanthan gum solutions: Steady shear flow behavior," *Fibers Polym.*, vol. 7, no. 2, pp. 129–138, Jun. 2006.

[16] E. R. Morris, A. N. Cutler, S. B. Ross-Murphy, D. a. Rees, and J. Price, "Concentration and shear rate dependence of viscosity in random coil polysaccharide solutions," *Carbohydr. Polym.*, vol. 1, no. 1, pp. 5–21, Sep. 1981.

[17] C. Castelain, J. L. Doublier, and J. Lefebvre, “A study of the viscosity of cellulose derivatives in aqueous solutions,” *Carbohydr. Polym.*, vol. 7, no. 1, pp. 1–16, Jan. 1987.
[18] P. Webb, “Volume and density determinations for particle technologists,” 2001.
[19] I. Oral, H. Guzel, and G. Ahmetli, “Measuring the Young’s modulus of polystyrene-based composites by tensile test and pulse-echo method,” *Polym. Bull.*, vol. 67, no. 9, pp. 1893–1906, Jun. 2011.
[20] E. Schreiber, O. L. Anderson, and N. Soga, *Elastic Constants and Their Measurement*. McGraw-Hill, 1973, pp. 1–7.
[21] W. Węglewski, K. Bochenek, M. Basista, T. Schubert, U. Jehring, J. Litniewski, and S. Mackiewicz, “Comparative assessment of Young’s modulus measurements of metal–ceramic composites using mechanical and non-destructive tests and micro-CT based computational modeling,” *Comput. Mater. Sci.*, vol. 77, pp. 19–30, Sep. 2013.
[22] NSG Group, Pilkington North America, “Properties of Soda-Lime-Silica Float Glass,” 2012.
[23] J. Kováčik, “Correlation between Young’s modulus and porosity in porous materials,” *J. Mater. Sci. Lett.*, vol. 8, pp. 1007–1010, 1999.
[24] K. O. Kese, Z. C. Li, and B. Bergman, “Influence of residual stress on elastic modulus and hardness of soda-lime glass measured by nanoindentation,” *J. Mater. Res.*, vol. 19, no. 10, pp. 3109–3119, Mar. 2011.

Author Biography

Michael Avery received his MSci in Chemical Physics with Industrial Experience from the University of Bristol (2012). He is currently a PhD student at the Bristol Centre for Functional Nanomaterials where he is researching new silica-based materials for 3D-printing.